

# Measurement of the polarisation in the auroral $N_2^+$ 427.8 nm band

Mathieu Barthelemy<sup>1,\*</sup>, Hervé Lamy<sup>2</sup>, Anne Vialatte<sup>1</sup>, Magnar Gullikstad Johnsen<sup>3</sup>,  
Gaël Cessateur<sup>2</sup>, and Naïma Zaourar<sup>4</sup>

<sup>1</sup> Univ. Grenoble Alpes, CNRS, IPAG, 38000 Grenoble, France

<sup>2</sup> Royal Belgian Institute for Space Aeronomy, Belgium

<sup>3</sup> Tromsø Geophysical Observatory, UiT the Arctic University of Norway, Norway

<sup>4</sup> USHB, Alger, Algeria

Received 31 March 2018 / Accepted 21 May 2019

**Abstract**—In this paper, we provide for the first time polarisation measurements of the  $N_2^+$  band at 427.8 nm performed with Premier Cru, a dedicated spectropolarimeter to investigate the polarisation of auroral emission lines between 400 and 700 nm. Details about the instrument, the observing conditions and the data analysis procedure are provided. Results obtained during three nights in March 2017 in Skibotn, Norway, indicate that the auroral blue line is polarised with a degree of linear polarisation of a few %. Due to weak Signal-to-Noise Ratios (SNR), these measurements still need to be taken with caution since none of the individual data set has a detection with a  $3\sigma$  confidence level. However, results integrated over the entire observing period each night do show a  $3\sigma$  detection but due to the long integration period, the origin of this polarisation cannot be linked to a specific type of aurora (diffuse vs structured arc) or specific ionospheric or geomagnetic conditions. These observations need to be confirmed with an improved design to increase the SNR and decrease the exposure time. When available, these improved measurements of the blue line polarisation will be important to better understand the physics of auroral processes at altitudes below 100 km where the  $N_2^+$  emission occurs and possibly for space weather applications if the polarisation varies with ionospheric/geomagnetic conditions.

**Keywords:** polarisation / aurora / space weather-ionosphere-instrumentation

## 1 Introduction

The polarization of the auroral 630 nm red line was discussed theoretically in Lilensten et al. (2006) then observationally confirmed by Lilensten et al. (2008) using a dedicated Steerable Photo Polarimeter (SPP). Subsequent observations (e.g., Barthelemy et al., 2011) confirmed that the red line is polarized at a level of 2–3% with significant variations on short time scales. This new observable could be useful either to monitor the response of the upper atmosphere to particle precipitations (Lilensten et al., 2015) or possibly to map the variations of the direction of the local magnetic field during geomagnetic activity (Lilensten et al., 2016). Polarization is always linked to some anisotropy, either in the emission process itself or along the line-of-sight. At high latitudes, in the case of the 630 nm oxygen red line, the polarization is due to the anisotropy of the precipitating electron beams impacting oxygen atoms, creating imbalances between the various (unresolved) Zeeman sublevels (Bommier et al., 2011).

The next logical step is then to check whether other auroral emission lines could also be polarized by impact with precipitating electrons. To try to answer this question, the Royal Belgian Institute for Space Aeronomy (BISA) and the Institute of Planetology and Astrophysics of Grenoble (IPAG) have partnered to design and build a spectropolarimeter (called Premier Cru), working in harsh conditions, with the goal to measure the polarization of the auroral emission lines between approximately 400 and 700 nm. Additionally, results from Premier Cru can also be used to confirm the measurements for the polarization of the red line previously obtained with SPP.

Among all the auroral emission lines, since the 577.7 nm green line cannot be polarized (Bommier et al., 2011), the best candidate is therefore the blue line at 427.8 nm, which corresponds to the 0–1 transition of the first negative band of  $N_2^+$  ( $B^2\Sigma_u^+ - X^2\Sigma_g^+$ ). Indeed, first, is it usually the third brightest auroral emission (although most of the time not visible with the naked eye). Since the excitation threshold of  $N_2^+$  is 18.75 eV, this band is almost permanently emitted in the auroral oval region, and is intense especially during geomagnetic activity. Second, it is produced by impact with precipitating electrons

\*Corresponding author: [mathieu.barthelemy@univ-grenoble-alpes.fr](mailto:mathieu.barthelemy@univ-grenoble-alpes.fr)

only, while the red line can also be produced by many isotropic competing mechanisms which do not produce polarization and therefore dilute it. Third, the blue line generally peaks at altitudes around or below 100 km and is therefore produced by energetic keV electrons (Rees, 1989). Hence, complementary information could be obtained from the measurement of the polarisation of the blue line since the emission peak altitude and the energy range of electrons at the origin of the emission are very different than in the case of the red line. Finally, the blue emission is restricted to a much thinner altitude range than the red line. This reduces the uncertainty on the position in the horizontal plane where the signal is coming from compared to the red line and might be important to link with the local magnetic field direction.

So far, no theoretical study of the blue line polarisation is available unlike for the red line (Bommier et al., 2011). Therefore, the magnitude and direction of polarisation for the blue line due to the impact with a precipitating collimated electron beam is unknown while for the red line, it was shown that the polarisation is oriented parallel to the local magnetic field line. Furthermore, an additional complication/difference comes from the rotational structure of the vibronic transition at 427.8 nm, which is only visible at high spectral resolution, well beyond what can be achieved with Premier Cru. In principle, each rovibronic line could have a different polarisation and what will be observed is the integrated value over the band. This paper is therefore exploratory with the aim to present preliminary results of the polarization measured in the full integrated 427.8 nm  $N_2^+$  band using Premier Cru during a campaign organized in March 2017 in northern Norway. Depending on the results, additional instruments with improved designs will be considered as well as the development of the theory of the blue line polarisation.

## 2 Observation campaign

### 2.1 The Premier Cru instrument

The Premier Cru instrument consists of two parts: a box controlled in temperature contains all the optics and is located outside, while the spectrograph/CCD camera is located inside the station. The box contains a C-8 Celestron telescope ( $f/D = 10$ ,  $D = 200$  mm) in order to collect the light, a lens to allow field pupil inversion, a rotating achromatic Half-Wave Retarder (HWR)<sup>1</sup>, a polarizing beam-splitter cube which splits the incident beam into two orthogonally-polarized extraordinary and ordinary beams separated by 90°. The beams are then transmitted to the spectrometer via two 600  $\mu\text{m}$  core optical fibers. The fibers are matched to the tunable slit of a Czerny-Turner 303 mm (Shamrock model) spectrometer which comprises three gratings with 300 l/mm, 600 l/mm and 1800 l/mm. A schematic of the instrument concept is shown on Figure 1. During the observations discussed in this paper, the size of the slit was 150  $\mu\text{m}$ , the grating used was the 300 l/mm, and the exposure time for each of the four positions of the HWR was 600 s meaning that a complete set is recorded every 2400 s (40 min). The Field of View (FoV) is approximately 0.6°.

The data are collected on a 1024  $\times$  255 CCD matrix (ANDOR IDUS camera) cooled down to  $-70^\circ\text{C}$ . A multi track mode with co-addition of 10 adjacent lines was used, providing a 1024  $\times$  25 data matrix as final result and increasing the Signal-to-Noise Ratios (SNR). Lines 1–12 are summed to compute intensities in the ordinary beam, while lines 14–25 correspond to intensities of the extraordinary beam. Line 13 is used as separation between the two beams and is not included in the measurement of the intensities.

### 2.2 Acquisition geometry

During the campaign in March 2017, the instrument was located at the Skibotn Fieldstation (69° 23' 27" N, 20° 16' 02" E) of the University in Tromsø (UIT, the Arctic University of Norway). It was constantly pointing to the same direction, with a 30° elevation and a 270° azimuth (geographic West). Since the measured polarisation of the red emission is maximal when the line of sight is perpendicular to the magnetic field line, this orientation is quite optimal as shown in Lilensten et al. (2016). Since the orientation of the polarisation for the blue line is unknown a priori, we conservatively decided to keep this orientation during the entire campaign. As shown in Figure 2, this provides an angle of 71.98° between the line-of-sight and the magnetic field at an altitude of 220 km and of 71.85° at an altitude of 85 km (lowest limit of the blue emission line). The distance between the instrument and the emission region is 167 km at 85 km altitude and 420 km at 220 km. Local magnetic field directions were computed using IGRF model 2000 (Olsen et al., 2000). With this geometry, the sine of  $\sim 71.8^\circ$  is  $\sim 0.95$  and therefore the measured polarisation of the red line is approximately 5% lower than the intrinsic value.

### 2.3 Data analysis: general procedure

We work with sets of eight spectra: the ordinary and extraordinary spectra provided by the beam splitter for each position angle of the HWR, namely 0°, 22.5°, 45°, and 67.5°. Since  $N_2^+$ , at 427.8 nm,  $O^1S$  at 557 nm and  $O^1D$  at 630 and 636 nm are lines easy to identify (Fig. 3), the spectra are calibrated in wavelength using a third order polynomial least square fit for the other lines. Many other lines can be observed in some spectra such as  $H_\alpha$  at 656 nm or the  $N_2$  first positive bands between 600 and 700 nm, especially when the geomagnetic activity increases. An example is shown in Figure 3.

The first step consists in defining a local continuum and setting the limits of the blue line in the ordinary and extraordinary spectra with the HWR at position angle 0° (hereafter called o00 and e00). With the grating and slit used, we cannot resolve any rotational structure within the blue line. The polarisation measurements are carried out by integrating the intensities over the whole band.<sup>2</sup> The same boundaries are then used to define the blue line in all the other six spectra acquired with the HWR set at other position angles. In the spectra, cosmic rays sometimes produce strong and sharp peaks (Fig. 3). They have been removed manually using a linear interpolation between the two sides of the cosmic ray trace.

The normalized Stokes parameters  $q$  and  $u$  and the Degree of Linear Polarization (DoLP) can then be calculated. Both the

<sup>1</sup> Model AHWP10M-600 from Thorlabs.

<sup>2</sup> Since the shape of the band is complex, no fit is performed.

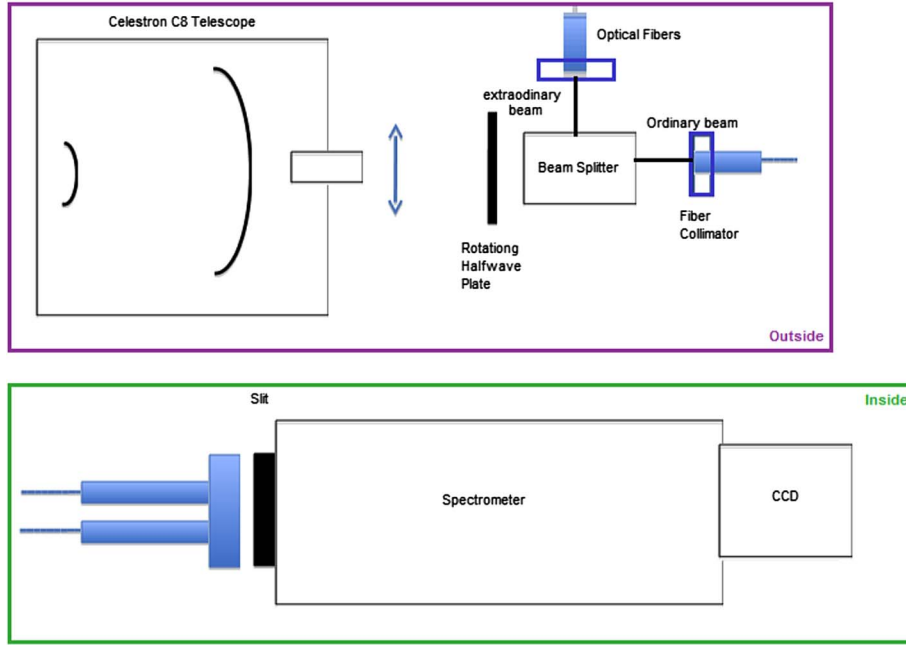


**Fig. 1.** Concept of the Premier Cru instrument. The purple part is in a box located outside while the green one is inside the adjacent observatory. A 50 m long and 600  $\mu\text{m}$  diameter double core optical fiber links the two parts.

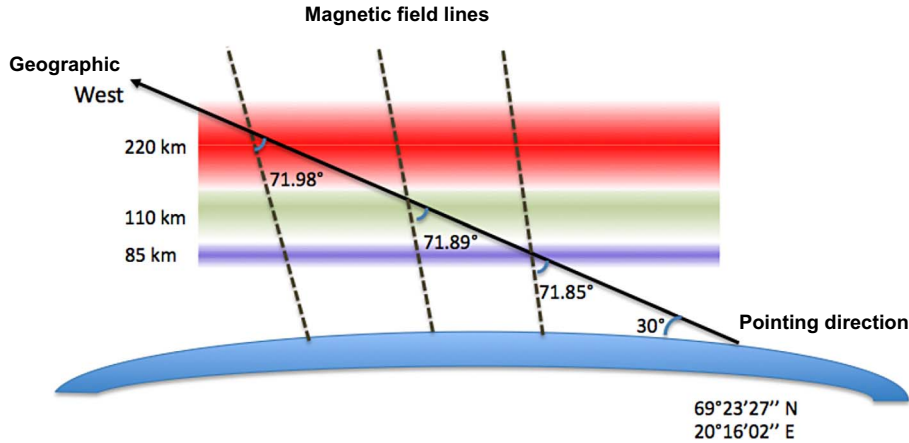


**Fig. 2.** Observation geometry during the campaign in Skibotn in March 2017.

ratio and the difference methods are used (as e.g., in Barthelemy et al., 2011 in the case of a similar optical design) in order to double check the whole procedure. The two methods are briefly reminded below. Note that since the HWR is achromatic, the correction due to the retardance variation over the spectrum can be neglected.

The following equations are used in the ratio method (Semel et al., 1993; Donati et al., 1997):

$$q = \frac{R_q - 1}{R_q + 1} \quad \text{and} \quad u = \frac{R_u - 1}{R_u + 1} \quad (1)$$

where  $R_q$  and  $R_u$  are the positive square roots of the following quantities.

$$R_q^2 = \frac{(I_{e0}/I_{o0})}{(I_{e45}/I_{o45})} \quad \text{and} \quad R_u^2 = \frac{(I_{e22.5}/I_{o22.5})}{(I_{e67.5}/I_{o67.5})} \quad (2)$$

The difference method is given by:

$$F_q = \frac{I_{e0} + I_{e45}}{I_{o0} + I_{o45}} \quad \text{and} \quad F_u = \frac{I_{e22.5} + I_{e67.5}}{I_{o22.5} + I_{o67.5}} \quad (3)$$

then

$$q = \frac{I_{e0} - I_{e45} - F_q(I_{o0} - I_{o45})}{I_{e0} + I_{e45} + F_q(I_{o0} + I_{o45})} \quad (4)$$

and

$$u = \frac{I_{e22.5} - I_{e67.5} - F_q(I_{o22.5} - I_{o67.5})}{I_{e22.5} + I_{e67.5} + F_q(I_{o22.5} + I_{o67.5})} \quad (5)$$

The ratio method compensates for a possible small difference between the transmissions of the ordinary/extraordinary

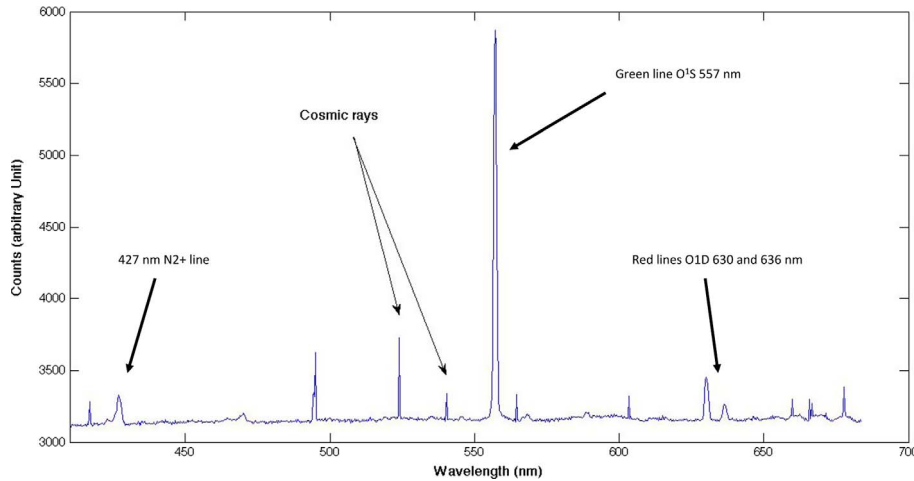


**Fig. 3.** Spectrum of the ordinary beam with the HWR position at  $0^\circ$  acquired on March 2, 2017 at 19:38. The cosmic rays mentioned in the text are the strong and thin peaks while the auroral lines are much wider due to the aperture of the slit. Two of them are pointed in the figure.

beams in the beam-splitter cube and in the fibers. Due to a possible misalignment of the optics in harsh conditions and the size of the fibers compared to the slit width, an additional difference of intensities between the ordinary and extraordinary spectra was observed and is corrected as well by the ratio method. However, they are not corrected in the difference method. Hence, to solve this issue, we rely on the fact that the green emission line at 577 nm cannot be polarized since the transition is quadrupolar. Therefore, for this particular line, the intensities integrated over the line in the two spectra should be identical. This allows us to compute a correction factor to compensate for the observed variation of intensities at this wavelength. Further, we apply this correction factor to the blue line at 427.8 nm assuming that the asymmetry between the spectra intensities is constant over the observed wavelength range. It also corrects for some possible instrumental polarisation which can occur despite the cylindrical symmetry of the instrument (e.g., due to reflections inside the polarising elements themselves). As above, it is assumed that this instrumental polarisation is constant over the entire spectrum.

DoLP is then obtained from

$$p = \sqrt{q^2 + u^2} \quad (6)$$

Uncertainties on the Stokes parameters are calculated by propagating the uncertainties on the line intensities due to photon noise which is dominant and the read-out noise<sup>3</sup> into equations (1)–(6). Since values in one of the spectra are corrected by a multiplicative factor (for each orientation angle of the HWR), an additional error could be introduced due to uncertainties in our estimate of the green line intensities in e00 and o00. However, since the SNR for the green line is always large ( $\sim 250$ ), the error introduced is always very small and negligible in regard to the other uncertainties.

Since the DoLP is the sum of two squared numbers, it is intrinsically biased by noise and the measured polarization is always larger than the true one. Simmons & Stewart (1985) proposed four methods to correct for this bias. In this paper, since

the goal is mostly to determine if the blue emission line is polarised and since we are dealing with relatively low SNR (30–100 depending of the band intensity), the maximum likelihood estimator is used. This estimator is the most severe one assuming that the true DoLP is equal to 0 when  $\frac{p}{\sigma_p} < 1.41$ , where  $\sigma_p$  is the uncertainty on the DoLP calculated from the noise obtained from the intensities and propagated in formulas (1)–(6).

## 3 Results

### 3.1 Selection of useful data

Most of the time, the blue line was visible in the spectra but too weak to provide a sufficiently high value of the SNR to compute the polarisation. Also sometimes, when the sky was a bit hazy, light from the small village of Skibotn at around 5 km from the fieldstation was scattered by thin clouds and clearly visible in the spectra as a very wide Na line from high pressure Sodium lamps.

Therefore, here we focus on three days (March 1, 2 and 5) during which the geomagnetic activity was strong (Kp index up to six) and auroral emissions were the most intense. As an example, the keogram obtained for the geographic North–South meridian with the All-Sky Camera (ASC) located next to the Skibotn fieldstation is shown at Figure 4a. This keogram illustrates that the auroral activity was very intense after  $\sim 18$  UT. Note that the FoV of Premier Cru is not visible in this keogram but the aurora covers the whole sky from Northern to Southern horizon, corresponding to a latitudinal width of the auroral oval of roughly 900 km. Since the scale length of the oval is larger in the East–West direction, it is reasonable to also assume that auroral activity was intense in our FoV as well during the observing period. The magnetogram measured in Tromsø (65 km away from the fieldstation) on March 5 is also shown in Figure 4b. During the period corresponding to our observations that night (roughly from 20:00 until 23:00 UT), the horizontal component of the magnetic field was most of the time below  $-400$  nT and sometimes reached values as low as  $\sim -800/-900$  nT.

<sup>3</sup>  $4 e^-$  in the ANDOR IDUS specifications.

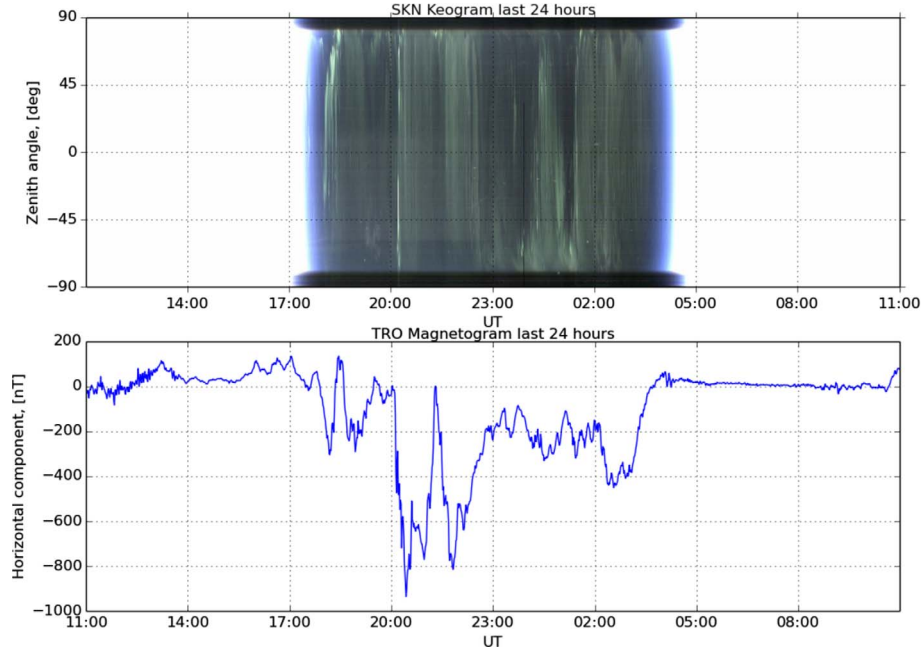


**Fig. 4.** (a) Keogram obtained for the geographic N–S meridian with the ASC located at the Skibotn Observatory on March 5, 2017, (b) horizontal component of the magnetic field recorded at the Tromsø observatory the same day. Both diagrams illustrate a very high auroral activity during the observations with Premier Cru.

**Table 1.** Results of the DoLP measurements during the three days in March 2017.

| Date       | Time LT  | $p_r$ (%) | $p_d$ (%) | $\sigma_{p_t}$ (%) | $p_r/\sigma_{p_t}$ | $p_{r0}$ (%) | $p_{r0}/\sigma_{p_t}$ | L |
|------------|----------|-----------|-----------|--------------------|--------------------|--------------|-----------------------|---|
| 01-03-2017 | 20:16:17 | 1.43      | 1.42      | 1.75               | 0.81               | 0            | 0                     | 3 |
| 01-03-2017 | 21:02:01 | 3.54      | 3.07      | 1.50               | 2.36               | 3.17         | 2.11                  | 2 |
| 01-03-2017 | 21:47:19 | 2.51      | 2.40      | 1.00               | 2.51               | 2.28         | 2.28                  | 1 |
| 01-03-2017 | 23:15:39 | 1.37      | 1.35      | 3.26               | 0.42               | 0            | 0                     | 1 |
| 01-03-2017 | All sets | 2.84      | 2.79      | 0.78               | 3.64               | 2.73         | 3.5                   | 2 |
| 02-03-2017 | 19:38:55 | 2.18      | 1.97      | 1.11               | 1.97               | 1.80         | 1.62                  | 4 |
| 02-03-2017 | 20:27:11 | 4.00      | 3.98      | 1.33               | 3.01               | 3.76         | 2.84                  | 1 |
| 02-03-2017 | 21:16:46 | 2.54      | 2.40      | 1.38               | 1.83               | 1.98         | 1.43                  | 2 |
| 02-03-2017 | 22:48:13 | 2.50      | 2.31      | 1.10               | 2.27               | 2.22         | 2.01                  | 2 |
| 02-03-2017 | 23:38:09 | 1.52      | 1.69      | 2.25               | 0.67               | 0            | 0                     | 1 |
| 02-03-2017 | All sets | 1.76      | 1.69      | 0.54               | 3.24               | 1.67         | 3.09                  | 2 |
| 05-03-2017 | 21:14:18 | 1.20      | 1.16      | 0.93               | 1.29               | 0            | 0                     | 3 |
| 05-03-2017 | 22:02:01 | 1.72      | 1.72      | 1.23               | 1.40               | 0            | 0                     | 4 |
| 05-03-2017 | 23:00:09 | 1.43      | 1.26      | 1.13               | 1.26               | 0            | 0                     | 3 |
| 05-03-2017 | All sets | 1.19      | 1.19      | 0.55               | 2.16               | 1.03         | 1.87                  | 3 |

Due to the presence of the Moon on March 5, an additional continuum was observed but could be easily removed and did not affect the signal from the aurora. This means that observations are possible even with moonlight which is not possible with a photometer such as SPP using a single wavelength channel.

In addition to analyses of individual sets of eight spectra, for the three active periods considered, a sum of all data sets available for each evening has been carried out to estimate an average polarisation during the entire period. Of course, in

this case, only long-term polarisation structure can be measured, preventing us to distinguish any variation of the polarisation with ionospheric conditions or detailed geomagnetic activity.

### 3.2 Polarisation results

Results for the three days in March are given in Table 1. It provides the date, start time of the observation sets, the DoLP measured with the ratio and difference methods (respectively

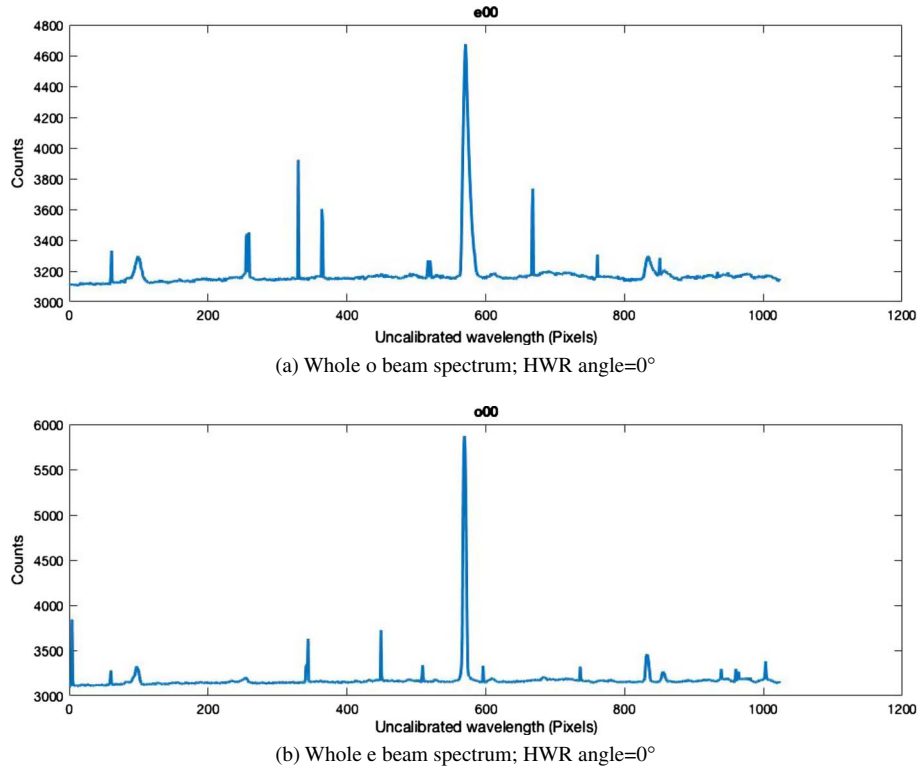


**Fig. 5.** Raw whole spectra for the data set taken March 2nd 2017 from 19:35 to 20:20. Calibration in wavelength is not shown since it is not used in the data processing once the blue line has been located. Both o (Left panels) and e (Right panels) beams are shown at HWR position  $0^\circ$ .

called  $p_r$  and  $p_d$ ), the uncertainty on the DoLP measured with the ratio method  $\sigma_{p_r}$ , the corresponding SNR  $p_r/\sigma_{p_r}$ , the debiased value of the DoLP  $p_{r_0}$  using the ratio method, and the corresponding SNR  $p_{r_0}/\sigma_{p_r}$ . Eventually a coefficient  $L$  is provided by the authors as a level of confidence from 1 (low) to 4 (very good) to take into account the cases where some complication occurs such as haze, thin clouds, cosmic ray traces on the edge of the lines, unexpected noise, etc. As an example, an entire data set (March 2nd from 19:38 to 20:20) is plotted on [Figures 5 and 6](#). For this data set the DoLP is  $1.97 \pm 1.11\%$  with the ratio method. The data set has almost no pixels with cosmic rays traces.

The values of the DoLP obtained with the ratio and the difference methods are very close to each other, which gives confidence in the results and in the computation of the correction factor using the fact that the green line is unpolarised. No polarisation at the  $3\sigma$  confidence level is detected in individual data sets. The highest value of  $p_{r_0}/\sigma_{p_r}$  is 2.84 but with a low level of confidence due to the presence of a large number of cosmic rays in that data set. If we do not consider the data sets with level of confidence 1 or 2, the highest SNR is only 1.62 with an unbiased value of the DoLP equal to 1.80%.

The debiased DoLP  $p_{r_0}$  ranges from 0% to 3.17%. Note that 0 does only mean that the debiasing method provides a polarisation compatible with 0 considering the noise in data. It does not mean that the polarisation is strictly equal to 0.

The DoLP measured when adding all the data sets of an evening presents a much better SNR. The polarisation level is not cancelled out when using long term integration and is still

measurable with a debiased DoLP ranging from 2.73% to 1.03%. Since the SNR is higher, detections with more than  $3\sigma$  are obtained for March 1 and 2. However, the level of confidence for these days is low and so these  $3\sigma$  detections have to be taken with care. Polarisation is smaller for March 5 with a value of  $p_{r_0}/\sigma_{p_r} = 1.87$  but with a higher confidence level ( $L = 3$ ).

### 3.3 Additional checks

A few additional checks can be done to give more confidence in these measurements. First is to compare with previous polarisation measurements on the auroral red line (630 nm). The results need to be in the same order of magnitude compared to the DoLP measurements on this line. This has been performed for the night of March 2nd. The DoLP in this case is  $4.6\% \pm 0.9\%$  with the ratio method which is in the same order of magnitude compared to previous measurements of the red line DoLP ([Lilensten et al., 2008, 2015](#)).

A last check of the results is done by performing some null parameter calculations ([Donati et al., 1997; Bagnulo et al., 2009](#)). Using the equations given by [Donati et al. \(1997\)](#) with the same data set (March 2nd), the absolute value of the normalized null parameter  $N/I$  is of the order of 0.52% which is less but not totally negligible compared to the measured Stokes parameter. It is however coherent with the observed noise in the measured Stokes parameters. The null parameter has been also calculated for the data set shown in [Figure 6](#). In this case  $|N/I|$  is equal to 0.39%.

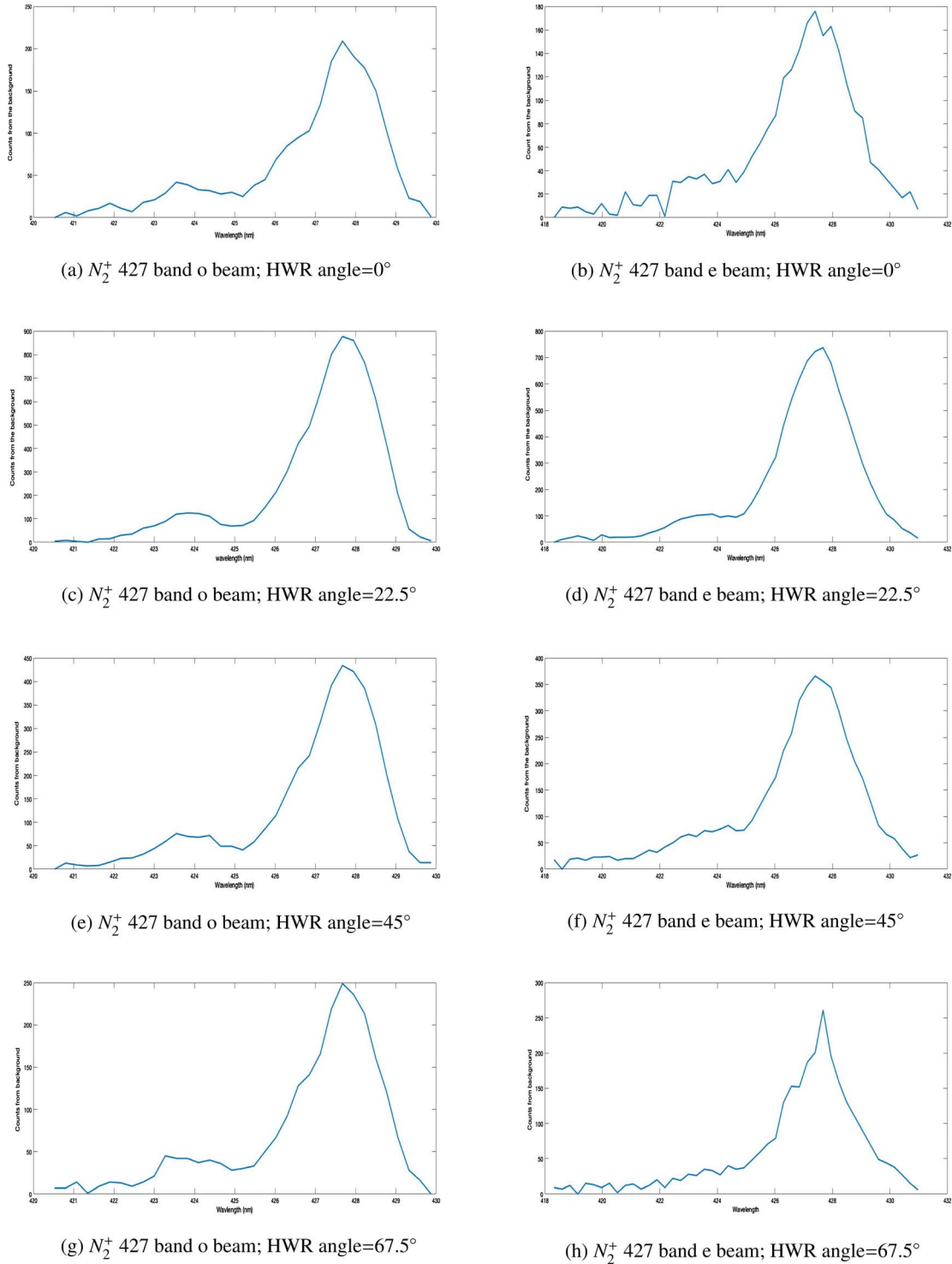


**Fig. 6.** Extracted blue line profile after background subtraction and cosmic rays traces removal for the data set taken March 2nd 2017 from 19:35 to 20:20. Both o (Left panels) and e (Right panels) beams are shown. Extraction is done using the method previously described in the paper. Integration is done using the shown profile. The line peak is at 427.8 nm.

## 4 Conclusion and discussion

We have carried out the first polarimetric measurements of the  $N_2^+$  band with a dedicated spectropolarimeter called Premier

Cru. The measured DoLP, integrated over the whole band, ranges from 1 to 4% but no measurement for individual data set corresponds to a detection with a  $3\sigma$  confidence level interval. For each of the three nights of observations, we have

co-added measurements from individual sets in order to increase the SNR. The results, corresponding to an integration of several hours, eventually provide detections at the  $3\sigma$  level. Due to this very long time averaging, these values must be treated with care as we may have integrated various auroral phenomena passing by in the FoV of the instrument. However, since the blue emission line was permanently emitted during these very active periods and since the resulting polarisation does not cancel out, this seems to indicate that the blue line is polarised at a certain level. Additional checks have been performed by calculating a null parameter for a night and by cross checking the red line polarisation. These measurements should be carried out again with improved instrumentation providing higher SNR and shorter integration time. A possibility could be to increase the FoV but this would then be obtained at the cost of spatial integration which could also average/decrease the polarisation. Another option could be to use a photomultiplier (PM) equipped with a narrow interference filter centered on the 427.8 nm band and a rotating polariser in front, using a design close to the one used for SPP (Lilensten et al., 2008). This PM must have a second channel equipped with an interference filter with the same width but slightly shifted in wavelength in order to measure and remove the possible light pollution background due e.g., to city lamps or moonlight.

If confirmed, the measurements of the blue line polarisation will allow to investigate the anisotropic processes occurring in the lowest part of the auroral region around or below 100 km altitude while the red line polarisation is probing these processes in a region near 220 km and upwards. In addition, contrary to  $O^1D$ , the  $N_2^+$  1NG band corresponds to an allowed transition with a short lifetime of the upper state. Hence, despite being at lower altitude, the depolarisation effect due to collisions will be much lower than for the red line. So the polarisation of the blue line should depend mostly on the ratio between primary and secondary electrons.

These measurements illustrate that impact with collimated precipitating electrons could potentially lead to polarisation in several auroral emission lines or bands and not only in the oxygen red line at 630 nm. In the future, several additional questions could be considered:

- What are the exact molecular processes at the origin of the polarisation of the 427.8 nm band? The results obtained here are an average over the entire band. Are every rotational line polarised the same way or are there differences? This would require a higher resolution instrument and ab initio calculation of the polarization mechanisms of the band through electron impact.
- Is the measured polarisation in the blue line related to some particular type of aurora? Is it due mostly to diffuse aurora or discrete arcs? Our current long-lasting averages do not allow us to answer this question.
- Are the other  $N_2^+$  bands like 0–0 band at 391 nm or the Meinel band polarised as well?
- How does the DoLP vary with ionospheric or geomagnetic parameters and could these polarisation measurements be useful for space weather applications?

*Acknowledgements.* This work was partially supported by grants from the OSUG@2020 labex, the PNST (French National program for Solar Terrestrial relation), the French Polar Institute IPEV (1026 Polarlis 2 project). The development of Premier Cru was mostly funded by the Solar Terrestrial Center of Excellence (STCE). The authors thank Anais James for her contribution during her intern from April to June 2016. The editor thanks Stefano Bagnulo and two anonymous referees for their assistance in evaluating this paper.

## References

- Bagnulo S, Landolfi M, Landstreet JD, Landi Degl'Innocenti E, Fossati L, Sterzik M. 2009. Stellar spectropolarimetry with retarder waveplate and beam splitter devices. *PASP* **121**: 993. DOI: [10.1086/605654](https://doi.org/10.1086/605654).
- Barthelemy M, Lystrup MB, Menager H, Miller S, Lilensten J. 2011. Is the Jovian auroral  $H_3^+$  emission polarised? *A&A* **530**: A139. DOI: [10.1051/0004-6361/201014314](https://doi.org/10.1051/0004-6361/201014314).
- Bommier V, Sahal-Bréchet S, Dubau J, Cornille M. 2011. The theoretical impact polarization of the O I 6300 Å red line of Earth aurorae. *Ann Geophys* **29**: 71–79. DOI: [10.5194/angeo-29-71-2011](https://doi.org/10.5194/angeo-29-71-2011).
- Donati J-F, Semel M, Carter BD, Rees DE, Collier Cameron A. 1997. Spectropolarimetric observations of active stars. *Mon Not R Astron Soc* **291**: 658. DOI: [10.1093/mnras/291.4.658](https://doi.org/10.1093/mnras/291.4.658).
- Lilensten J, Barthélemy M, Besson G, Lamy H, Johnsen MG, Moen J. 2016. The thermospheric auroral red line Angle of Linear Polarization. *J Geophys Res (Space Phys)* **121**: 7125–7134. DOI: [10.1002/2016JA022941](https://doi.org/10.1002/2016JA022941).
- Lilensten J, Bommier V, Barthélemy M, Lamy H, Bernard D, Idar Moen J, Johnsen MG, Løvhaug UP, Pitout F. 2015. The auroral red line polarisation: Modelling and measurements. *J Space Weather Space Clim* **5(27)**: A26. DOI: [10.1051/swsc/2015027](https://doi.org/10.1051/swsc/2015027).
- Lilensten J, Moen J, Barthélemy M, Thissen R, Simon C, Lorentzen DA, Dutuit O, Amblard PO, Sigernes F. 2008. Polarization in aurorae: A new dimension for space environments studies. *Geophys Res Lett* **35**: L08804. DOI: [10.1029/2007GL033006](https://doi.org/10.1029/2007GL033006).
- Lilensten J, Simon C, Barthélemy M, Moen J, Thissen R, Lorentzen DA. 2006. Considering the polarization of the oxygen thermospheric red line for space weather studies. *Space Weather* **4**: S11002. DOI: [10.1029/2006SW000228](https://doi.org/10.1029/2006SW000228).
- Olsen N, Sabaka TJ, Tøffner-Clausen L. 2000. Determination of the IGRF 2000 model. *Earth Planets Space* **52**: 1175–1182. DOI: [10.1186/BF03352349](https://doi.org/10.1186/BF03352349).
- Rees MH. 1989. *Physics and chemistry of the upper atmosphere*. Cambridge University Press. DOI: [10.1017/CBO9780511573118](https://doi.org/10.1017/CBO9780511573118).
- Semel M, Donati J-F, Rees DE. 1993. Zeeman-Doppler imaging of active stars. 3: Instrumental and technical considerations. *A&A* **278**: 231–237.
- Simmons JFL, Stewart BG. 1985. Point and interval estimation of the true unbiased degree of linear polarization in the presence of low signal-to-noise ratios. *A&A* **142**: 100–106.

**Cite this article as:** Barthelemy M, Lamy H, Vialatte A, Johnsen MG, Cessateur G, et al. 2019. Measurement of the polarisation in the auroral  $N_2^+$  427.8 nm band. *J. Space Weather Space Clim.* **9**, A26.